Huang, S., Zuo, W., Sohn, M. "Improved Cooling Tower Control of Legacy Chiller Plants by Optimizing the Condenser Water Set Point," *Building and Environment*, 111, pp. 33-46, 2017.

Improved Cooling Tower Control of Legacy Chiller Plants by Optimizing the Condenser Water Set Point

Sen Huang [a+], Wangda Zuo [a,*], Michael D. Sohn [b]

[a] *Department of Civil, Architectural and Environmental Engineering, University of Miami, 1251 Memorial Drive, Coral Gables, FL 33146, U.S.A.*
[b] *Energy Analysis and Environmental Impacts Division, Lawrence Berkeley National Laboratory, 1 Cyclotron Road, Berkeley, CA 94720, U.S.A.*
[+] *Current Address: Electricity Infrastructure and Buildings Division, Pacific Northwest National Laboratory, 902 Battelle Boulevard, WA 99354, U.S.A.*

Abstract:

Achieving the optimal control of cooling towers is critical to the energy-efficient operation of current or legacy chiller plants. Although many promising control methods have been proposed, limitations in their applications exist for legacy chiller plants. For example, some methods require the change of the plant's overall control structure, which can be difficult to legacy chiller plants; some methods are too complicated and computationally intensive to implement in old building control systems. To address the above issues, we develop an operational support system. This system employs a model predictive control scheme to optimize the condenser water set point and can be applied in chiller plants without changes in the control structure. To further facilitate the implementation, we propose to increase the optimization accuracy by selecting a better starting point. The results from a case study with a real legacy chiller plant in Washington D.C. show that the proposed operational support system can achieve up to around 9.67% annual energy consumption savings for chillers and cooling towers. The results also show the proposed starting point selection method can achieve a better accuracy and a faster computational speed than commonly used methods. In addition, we find that we can select a lower optimization frequency for the studied case since the impact of the optimization frequency on the energy savings is not significant while a lower optimization frequency does reduce the computational demand to a great extent.

* Corresponding author: w.zuo@miami.edu

Keywords: Model Predictive Control; Condenser Water Set Point; Optimization Starting Point; Optimization Frequency; Modelica

Nomenclature

t	Time
$E\|_{t_0}^{t_0+\Delta t}$	Energy consumption during the optimization period $[t_0, t_0 + \Delta t)$
P	Power
T	Temperature
$\dot{Q}$	Cooling load
$\vec{S}$	State vector
PLR	Part load ratio
COP	Coefficient of performance
ε	Effectiveness
c	Constant coefficient
y	Cooling tower fan speed ratio

Superscript

P	Predicted
$*$	With error

Subscript

cw	Condenser water
chw	Chilled water
set	Set point
wb	Outdoor wet bulb temperature
L	Low limit
H	High limit
low	The lowest possible value
hig	The highest possible value
tw	Cooling tower

ch	Chiller
ent	Entering the chiller
lea	Leaving the chiller
sta	Starting point
app	Approach
nom	Nominal
eva	Evaporator
con	Condenser
$staerr$	Static error

1. Introduction

Chiller plants are widely used to provide cooling to buildings [1]. As a result, about 5.17×10^{11} MJ annual energy consumption in the commercial buildings is attributed to chillers alone, which are the key components of chiller plants [1]. Including other components, such as cooling towers and pumps, the total energy consumption by chiller plants is even higher. Thus, it is necessary to enhance the energy efficiency of chiller plants.

Depending on how chillers reject the waste heat, chiller plants can be categorized as water-cooled and air-cooled. Water-cooled chiller plants with cooling towers are commonly used for large buildings. A typical water-cooled chiller plant consists of two water loops: a chilled water loop and a condenser water loop. The chilled water loop transfers the cooling energy generated by the chiller to the demand side; the condenser water loop rejects the waste heat from the chiller to the ambient environment through the water evaporation occurs in cooling towers [2].

Water-cooled chiller plants are typically controlled by a two-level control structure. The low-level control (local controller) is enabled by a feedback control system. For instance, the temperature of the condenser water leaving the cooling towers is typically controlled by adjusting the speed of the cooling tower fans to meet a predefined set point, which is referred as condenser water set point. The upper-level control (supervisor controller) is used to specify set points for the local controller and other time-dependent modes of operation [2]. Conventionally, set points are fixed at the nominal values.

One commonly used approach to improve energy efficiency of chiller plants is to optimize the control of the cooling towers: one can reduce chiller energy consumption by increasing cooling tower fan speeds so that the temperature of the condenser water entering the chillers is reduced. However, higher fan speeds mean that cooling towers will use more energy. Thus, the goal is to minimize the total energy consumption of cooling towers and chillers by adjusting the fan speeds of cooling towers.

Due to the nonlinear nature of chiller plant energy use, identifying the optimal cooling tower fan speed is challenging. For example, the energy performance curves of chillers and cooling towers are usually nonlinear and sometimes non-convex, which means the commonly used system analysis tools, such as linear optimization methods, may not be suitable for this problem. In addition, according to the ASHRAE Handbook [2], the optimal fan speeds of cooling towers may be affected by both the cooling load and weather conditions. Therefore, finding optimal cooling tower fan speed is also a multiple-input problem.

* Corresponding author: w.zuo@miami.edu

The current methods for optimizing cooling tower fan speeds [3-13] can be categorized into two groups. In the first group, researchers [3, 4] proposed to replace the two-level control structure by directly controlling the fan speeds according to cooling load conditions. For example, Braun, Klein, et al. [3] proposed a systematic method to control speeds of the variable-speed cooling tower fans: all the cooling tower fans should be operated with the same speed and a linear equation was proposed to determine the optimal fan speed according to the cooling load. This method is easy to implement and can make cooling tower control more stable.

In the second group, researchers [5-13] proposed to reset the condenser water set point according to the weather and/or cooling load conditions. Some researchers [5-8] have proposed near-optimal solutions in order to reduce computational runtimes and simplify the implementation. In the near-optimal solution, regression models are used to describe the relationship between the optimal condenser water set point and the wet bulb temperature, and/or cooling load conditions. The regression models are usually a linear regression model [5] [7] or a polynomial regression model [6] to facilitate the implementation in a real controller. Although simple, those regression models may lead to significant deviation from the real optimal results [2, 10]. Other researchers [9-12] developed model-based optimization methods to increase the optimization accuracy. For example, Lu, Cai, et al. [9] proposed to model the studied chiller plant with an empirical model and optimize the system by using a genetic algorithm to find the optimal condenser water set point. They found that they could save approximately 10% of the energy consumption for the studied condenser water loop during high load periods compared to the baseline in which cooling tower fans and condenser water pumps were always at full speeds.

However, above methods are not often suitable for legacy chiller plants. The methods in the first group may not be applied in legacy chiller plants due to the difficulties in changing the control structure of the legacy chiller plants. The control systems of the legacy chiller plants are usually enclosed and any modification can be difficult and uneconomical. For the methods in the second group, the most promising model-based optimization methods are usually highly complicated and computationally intensive. For legacy chiller plants, the existing control systems are commonly simple programmable logic controllers with limited computational resources available, which makes the implementation of model-based optimization methods very challenging.

Another operational constraint in legacy systems is that changing the condenser water set point cannot be performed very often since resetting may have to be done manually by the building operators. Therefore, identifying an appropriate resetting frequency for changing the condenser water set point is critical. On one side, a low resetting frequency can reduce efforts by the building operators. On the other side, a low frequency may reduce the energy savings due to the failure in capitalizing on the system dynamics; in addition, a lower optimization frequency leads to a longer prediction horizon for model inputs. The prediction accuracy will be likely decreased with a longer prediction horizon [14], which means more uncertainties will be introduced into the optimization. Thus, it is important to quantitatively evaluate the impact of the optimization frequency on the energy consumption by chiller plants.

This study attempts to develop an operational support system to optimize cooling tower operation for legacy chiller plants. Our system uses the predicted cooling load and wet bulb temperature as inputs for a model predictive scheme to search the optimal condenser water set points for a future period. The operators can then manually change the set points in the chiller control system, which alleviates the difficulty in the implementation for legacy building systems as it does not require the deployment of the algorithms in existing legacy controllers. To improve the optimization accuracy and increase the optimization speed, we also proposed an approach temperature based method for the selection of optimal search starting point. The proposed method was then assessed using a case study on a legacy chiller plant located in Washington D.C. In this case study, the energy saving is estimated based on offline simulations. To quantify the impact of set points changing frequency on the energy savings, we also evaluated the energy savings with different optimization frequencies in the case study.

Compared to the existing literature, this study makes the following contributions: first, we proposed an operational support system to optimize the cooling tower operation for legacy chiller plants, which is easier to implement than existing methods. Second, an approach temperature based method for selecting the starting point was developed to improve the accuracy and increase the speed of the model-based condenser water set point optimization. The approach temperature based method demonstrated a better performance compared to three commonly used methods. Third, we presented a systematic evaluation for the impact of the optimization frequency on the energy savings by the condenser water set point optimization. The evaluation can help operators determine the optimal resetting frequency.

2. Model Predictive Control for Optimizing the Condenser Water Set Point

2.1 Optimization Problem Definition

For the condenser water set point optimization, we consider a water-cooled chiller plant with multiple chillers and multiple cooling towers. The primary chilled water pumps and condenser water pumps are constant speed pumps. For each cooling tower, there is a variable speed fan controlled by one condenser water set point. We assume that all the cooling towers are controlled by the same condenser water set point and there is no other independent variable in the optimization. Since the change of the condenser water set point doesn't affect the operation of pumps, the optimization problem can be defined as

$$\underset{T_{cw,set}(t_0)}{\operatorname{argmin}}\left(E_{tot}\big|_{t_0}^{t_0+\Delta t}\right) = \min\left(\int_{t_0}^{t_0+\Delta t} (P_{ch}(t) + P_{tw}(t))dt\right) \tag{1}$$

for $t \in [t_0, t_0 + \Delta t)$

$$P_{ch}(t) = f(T_{cw,ent}(t), \dot{Q}^P(t), \vec{S}_{ch}(t)) \tag{2}$$

$$P_{tw}(t) = f(T_{wb}^P(t), T_{cw,set}(t_0), T_{cw,lea}(t), \vec{S}_{tw}(t)) \tag{3}$$

s.t.

$$T_{cw,set,L} \leq T_{cw,set}(t_0) \leq T_{cw,set,H}, \tag{4}$$

$$T_{cw,ent}(t) = f(T_{wb}^P(t), T_{cw,set}(t_0), T_{cw,lea}(t), \vec{S}_{tw}), \tag{5}$$

$$T_{cw,lea}(t) = f(\dot{Q}^P(t), P_{ch}(t), T_{cw,ent}(t), \vec{S}_{ch}), \tag{6}$$

where $E_{tot}\big|_{t_0}^{t_0+\Delta t}$ is the total energy consumption of the chillers and cooling towers during the optimization period $[t_0, t_0 + \Delta t)$, P_{ch} is the power of the chillers while P_{tw} is the power of the cooling towers, $T_{cw,set}$ is the condenser water set point, $\dot{Q}^P$ is the predicted cooling load over $[t_0, t_0 + \Delta t)$, T_{wb}^P is the predicted wet bulb temperature over $[t_0, t_0 + \Delta t)$, $T_{cw,ent}$ and $T_{cw,lea}$ are the temperature of the condenser water entering and leaving the chillers, respectively. $\vec{S}_{ch}$ and $\vec{S}_{tw}$ are the state vectors of the chillers and the cooling towers (e.g. equipment operating status, water temperature in chiller condenser and evaporator), respectively. $T_{cw,set,L}$ and $T_{cw,set,H}$ are the low and high limits of the condenser water set point during $[t_0, t_0 + \Delta t)$. Using the evaporative cooling, the cooling tower cannot cool the condenser water to a temperature lower than the outdoor web bulb temperature, T_{wb}. Thus, the actual $T_{cw,set,L}$ can be determined by

$$T_{cw,set,L} = minimum\{T_i \in \{T_1, \dots, T_n\} \mid T_i \geq T_{wb,L}^P\}, \tag{7}$$

where $\{T_1, \dots, T_n\}$ is the set of all the possible values for the condenser water set point, $T_{wb,L}^P$ is the lowest T_{wb}^P during $[t_0, t_0 + \Delta t)$. The $T_{cw,set,H}$ is set as

$$T_{cw,set,H} = maximum\,\{T_1, \dots, T_n\}\,. \tag{8}$$

In addition, $\dot{Q}^P$ can be estimated using the load prediction model shown in [15] and $T_{wb}^P(t)$ can be obtained from the weather forecast service.

2.2 Optimization Framework for Chiller Plants

To implement the optimization described in the section 2.1, we developed a framework for the chiller plant controls optimization. The core of the framework is a system model of the studied chiller plant and an optimization engine. The plant model can be re-initialized during the runtime for continuous optimization.

In addition, Python scripts are developed to automate the pre-processing, optimization and post-processing processes.

Figure 1 shows the workflow of the developed framework for the condenser water set point optimization. For the optimization period starting from t_0, the $\dot{Q}^P(t)$, ${T_{wb}}^P(t)$ and $\vec{S}(t_0)$ are used as input variables to perform the optimization, then the generated optimum $T_{cw,set}(t_0)$ would be used to obtain $\vec{S}(t_0+\Delta t)$ which would be used in the optimization for the next optimization period starting from $t_0+\Delta t$.

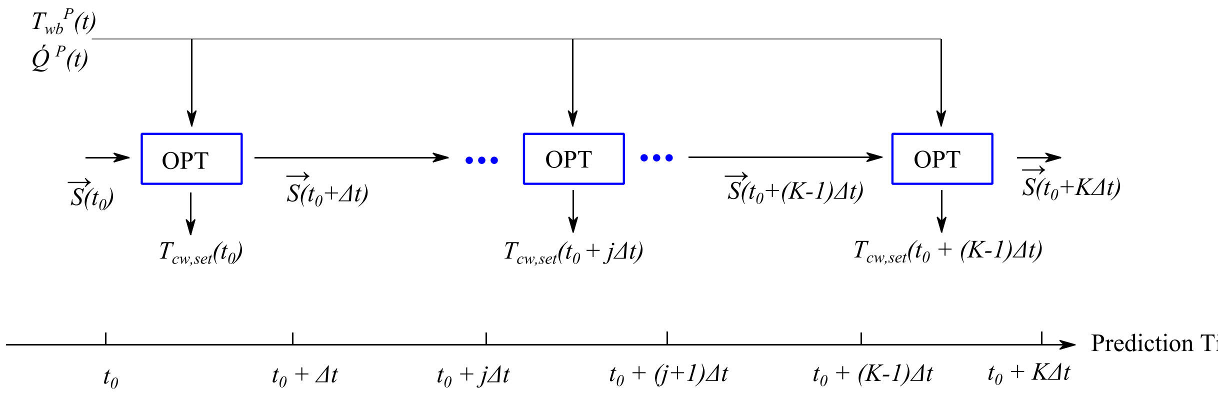

Figure 1 The workflow of the condenser water set point optimization

3. Starting Point Selection for the Condenser Water Set Point Optimization

In general, a good search starting point can significantly increase the success rate of finding the global optimum and reduce the searching time. For the condenser water set point optimization, finding the global minimum can be a critical issue since many local minima exist. The optimization algorithm can potentially be trapped in local minima if the starting point is not appropriately selected. In the following sessions, we will first introduce the local minima problem in the condenser water set point optimization. Then we will discuss benefits and difficulties of three typical methods for selecting the optimization starting point. Finally, we propose a new method, which is simple and effective.

3.1. Local Minima Problem

As shown in Figure 2, it is possible that $E|_{t_0}^{t_0+\Delta t}$ is constant if $T_{cw,set}$ is within a certain range (we name this range as "flat range"). When $\dot{Q}$ or T_{wb} is high, the flat range will occur at the lower end of $T_{cw,set}$ (Figure 2a). In this case,

$$T_{cw,low} \geq T_{cw,set,L}, \tag{9}$$

where $T_{cw,low}$ is the lowest possible temperature of the condenser water leaving the cooling tower when the cooling tower fans are running at full speeds. Thus, when $T_{cw,set} < T_{cw,low}$, we always have

$$E_{tw}|_{t_0}^{t_0+\Delta t} = contant, \qquad T_{cw,set} \in \left[T_{cw,set,L}, T_{cw,low}\right], \tag{10}$$

$$T_{cw,ent} = T_{cw,low}, \qquad T_{cw,set} \in \left[T_{cw,set,L}, T_{cw,low}\right], \tag{11}$$

where $E_{tw}|_{t_0}^{t_0+\Delta t}$ is the energy used by the cooling towers. With a constant $T_{cw,ent}$, the chiller energy consumption, $E_{ch}|_{t_0}^{t_0+\Delta t}$, will also remain unchanged. Thus, we will also have

$$E_{tot}|_{t_0}^{t_0+\Delta t} = contant, \qquad T_{cw,set} \in \left[T_{cw,set,L}, T_{cw,low}\right]. \tag{12}$$

When $\dot{Q}$ or T_{wb} is low, the flat range may occur at the higher end of $T_{cw,set}$ (Figure 2b). Under this condition, we will have

$$T_{cw,hig} \leq T_{cw,set,H}, \tag{13}$$

where $T_{cw,hig}$ is the highest possible temperature of the condenser water leaving the cooling tower when the cooling tower fans are off and only natural cooling happens. Thus, the cooling tower energy is zero:

$$E_{tw}|_{t_0}^{t_0+\Delta t} = 0, \qquad T_{cw,set} \in \left[T_{cw,hig}, T_{cw,set,H}\right]. \tag{14}$$

And we will also have

$$T_{cw,ent} = T_{cw,hig}, \text{and } E_{ch}|_{t_0}^{t_0+\Delta t} = constant,\ T_{cw,set} \in \left[T_{cw,hig}, T_{cw,set,H}\right]. \tag{15}$$

As a result, the total energy consumption of chillers and cooling towers is also constant:

$$E_{tot}|_{t_0}^{t_0+\Delta t} = constant,\ T_{cw,set} \in \left[T_{cw,hig}, T_{cw,set,H}\right] \tag{16}$$

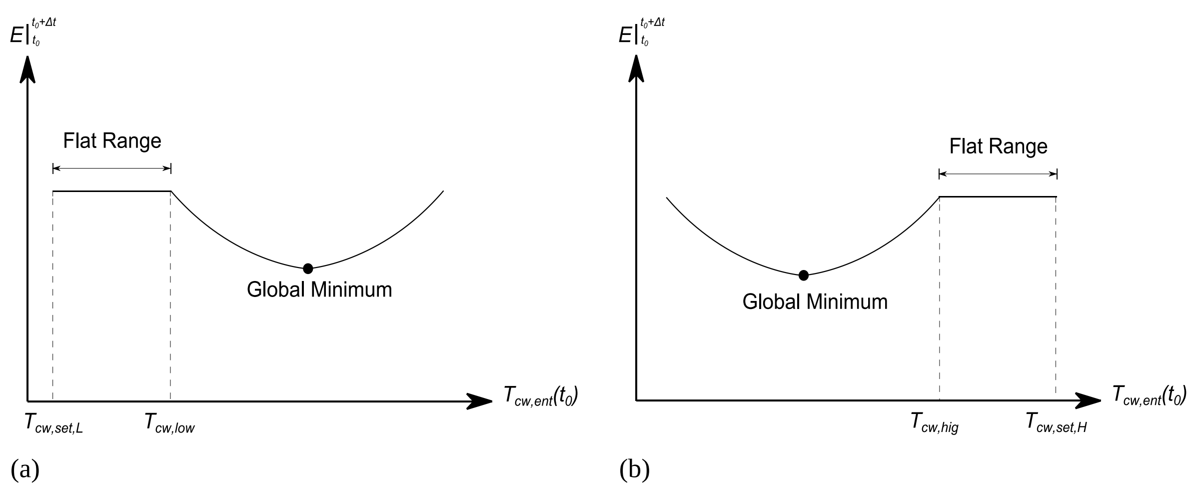

Figure 2 Flat ranges in the condenser water set point optimization

In both scenarios, the optimization algorithm will obtain a minimal solution in the flat range since it cannot detect any changes of $E_{tot}|_{t_0}^{t_0+\Delta t}$ for any $T_{cw,set}$ within the flat range. However, the obtained minimal solution is only valid for the flat range (local minimum).

3.2. Current Methods for Selecting Starting Point

To mitigate the local minima problem in the condenser water set point optimization, it is critical to start the search outside the flat range. Unfortunately, generic starting point selection methods, such as the middle point method, the multiple starting point method, and the previous value method may not be well-suited for avoiding the flat range problem.

The middle point method uses the middle point between the low bound and high bound of the independent variable as the starting point. Because it is the simplest method to reduce the distance of the starting point and the global minimum, the middle point method is widely used in optimization problems when only one global minimum is believed to exist [16, 17]. However, for the optimization problem with multiple local minima, the middle point method may lead to a local minimum if the local minimum is near the middle point.

As an improvement of middle point method, a multiple starting point method was proposed [18]. In this method, multiple starting points are generated randomly from a uniform distribution between the low and high bounds for the independent variable to increase the possibility that starting points are close to the global minimum. However, it still does not guarantee the global minimum and may increase the searching time with multiple starting points [19].

Alternatively, the previous value method [20] uses the optimal value resulted from the previous search as the starting points of the present search. The previous value method is based on the assumption that the optimal results for two adjacent optimization periods are likely close if the system states and inputs are similar. However, it may not work properly if the system states and inputs of two optimization periods are significantly different.

Specifically for the condenser water set point optimization, we can also use the highest possible set point as the starting point, $T_{cw,set,sta}$:

$$T_{cw,set,sta} = T_{cw,set,H}. \tag{17}$$

This method can be called as "high point" method. It can mitigate the flat range problem at the low end (Figure 2a) but not the one at the high end (Figure 2b).

3.3. Approach Temperature Method

To address the limitation of the current starting point selection methods for the condenser water set point optimization, we propose an approach temperature based method by considering the physics of the chiller plant. To avoid the flat range, $T_{cw,set,sta}$ should satisfy

$$T_{cw,set,sta} \in [T_{cw,low}, T_{cw,hig}]. \tag{18}$$

The challenge is how to predict $T_{cw,low}$ and $T_{cw,hig.}$ Although some sophisticated cooling tower performance models [21, 22] can be used to predict $T_{cw,low}$ and $T_{cw,hig}$, they are too complicated for the starting point selection. In this study, we propose to estimate the $T_{cw,low}$ based on the nominal approach temperature $\Delta T_{app,nom}$, which is the difference between the temperature of condenser water leaving the cooling tower and the wet bulb temperature at the nominal condition. The predicted $T_{cw,low}$ will be:

$$T_{cw,low}^{P} = \begin{cases} T_{cw,set,L} & T_{wb} < T_{cw,set,L} - \Delta T_{app,nom} \\ T_{cw,set,H} & T_{wb} > T_{cw,set,H} - \Delta T_{app,nom} \\ round\ (T_{wb} + \Delta T_{app,nom}) & Others \end{cases}, \tag{19}$$

where $round()$ is the function shown as follows:

$$round(T) = max\ \{T_i \in \{T_1, \ldots, T_n\} \mid T_i \leq T)\}, \tag{20}$$

where $\{T_1, \ldots, T_n\}$ is the set of all the possible values for $T_{cw,set}$ defined in equation (7). We then set:

$$T_{cw,set,sta} = T_{cw,low}^{P}, \tag{21}$$

It is worth mentioning that under certain conditions [23], it is possible that

$$\Delta T_{app} > \Delta T_{app,nom}, \tag{22}$$

where ΔT_{app} is the actual approach temperature. This will lead to

$$T_{cw,set,sta} = T_{cw,low}^{P} < T_{cw,low}. \tag{23}$$

In this case, the condition defined in (14) is no longer met and $T_{cw,set,sta}$ will be located in the flat range.

4. Case Study

To evaluate the performances of the proposed system and starting point selection methods, as well as to identify how optimization frequency affects the condenser water set point optimization, we implemented the proposed model predictive control in a real chiller plant. Then we performed an offline optimization using the historical cooling load and wet bulb temperature data as the inputs. The results are also reported in this section.

4.1 Case Description

The studied chiller plant is located in Washington D.C., U.S.A. The chiller plant has a primary-secondary chilled water distribution loop and our optimization focused on the primary loop. As shown in Figure 3, the chiller plant consists of three identical chillers, three identical cooling towers, three identical primary chilled water pumps, and three identical condenser water pumps. The chiller capacity is 970 ton. Each chiller has one dedicated chilled water pump, one dedicated condenser water pump, and one dedicated cooling tower. The temperature of chilled water leaving the chiller, $T_{chw,lea}$, is set as 3.89°C. The campus we studied had a legacy HVAC system and the AHU units could only handle chiller water at around 3.89°C. The cooling tower has a nominal fan power as 37 kW, the nominal wet bulb temperature, $T_{wb,nom}$, is 25.56°C and $\Delta T_{app,nom}$ is 3.89 K. A local controller is used to modulate the speeds of the cooling tower fans to maintain the temperature of the condenser water leaving the cooling towers as 29.44°C. In the condenser water loop, a three-way valve is employed to modulate the condenser flow rates through the cooling towers so that $T_{cw,ent}$ is not less than 15.00°C, which is the lowest temperature can be accepted by the chillers.

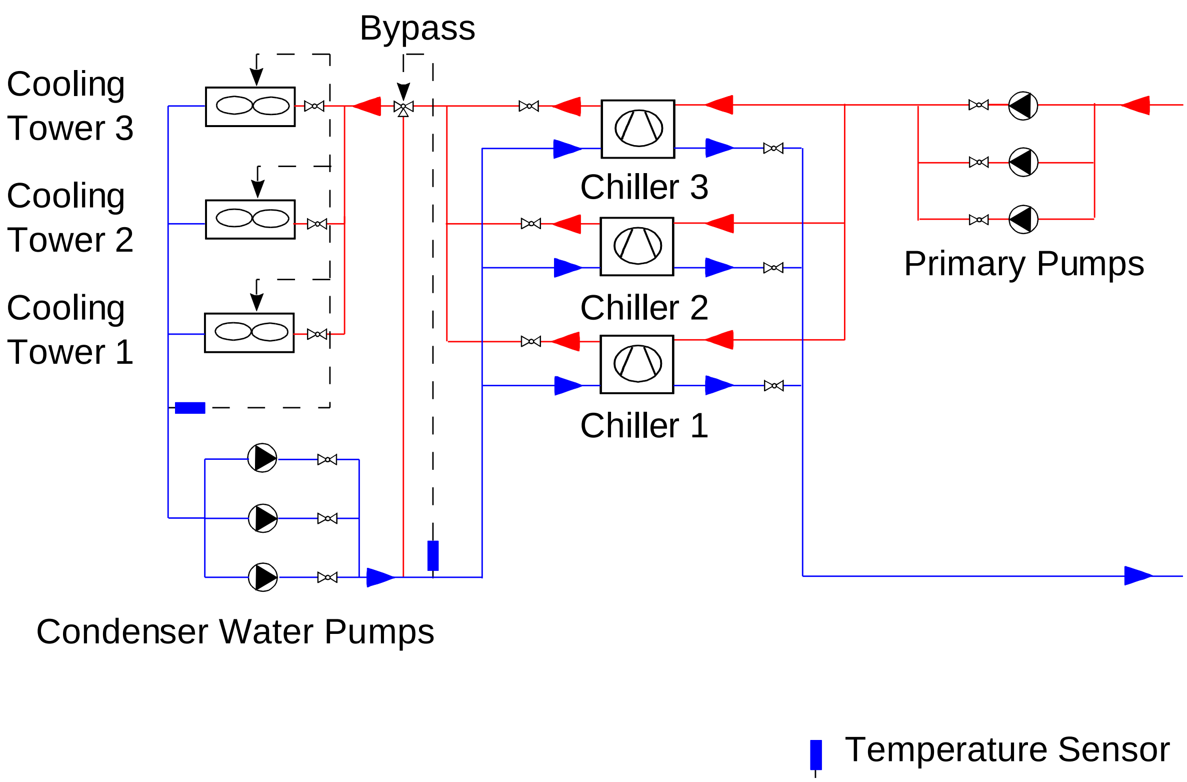

Figure 3 The schmatic of the studied chiller plant (the primary loop)

A supervisor controller is used to control the chiller operation status according to the measured cooling load. As described in Figure 4, there are four operating states for the chiller plant. For instance, “One On” means there is only one chiller in operation. The three chillers can be turned on or off sequentially. A chiller should not be turned on/off unless the measured cooling load is larger/smaller than a certain critical point plus/minus a dead band, such as 50 ton. The critical points are defined as 90.00% of the sum of the operating chillers' nominal cooling capacity. Besides the dead-band, a waiting period of 900 s is also applied to avoid chiller short cyclings.

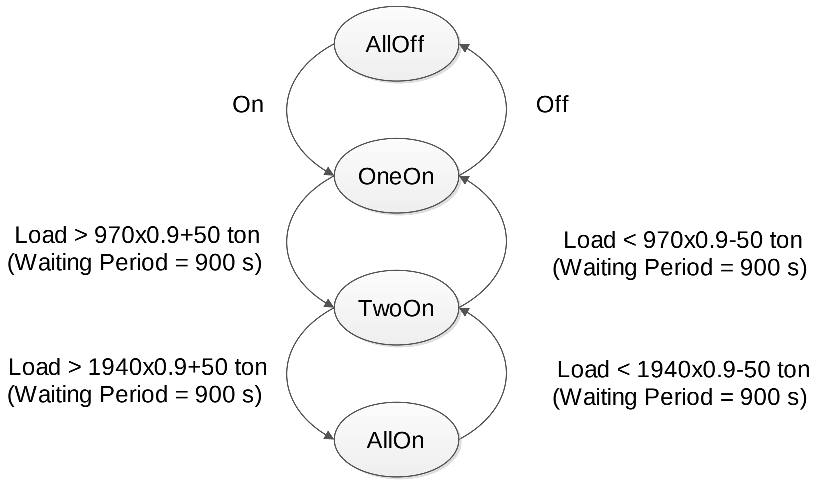

Figure 4 The state graph for the supervisor controller

4.2 Plant Models

In this study, we used Modelica to model the plant performance. Examples of building related modeling with Modelica include the modeling of building envelopes, a data center cooling system, and a chiller plant [12, 24-26].

We modeled the chiller plant using component models from Modelica *Buildings* library [24] and the state graph described in Figure 4 with the *Modelica_StateGraph2* library [27]. Modelica models were created and compiled with a commercial Modelica environment Dymola [28]. A hierarchical model structure has been applied and Figure 5 shows the top-level model, which represents the schematic in Figure 3. The subsystems for *Chillers*, *Cooling Towers with Bypass* and so on are packaged as single component models in the top-level model. Since our study focused on the primary loop, we prescribed the cooling load at the secondary loop using a *Cooling Load* model. Different than the system schematic, the top-level model also includes the control system, such as the *Supervisor Controller* model. The solid lines represent the pipes and the dashed lines are the paths for control signals and other inputs for the simulation, such as weather data and cooling load data.

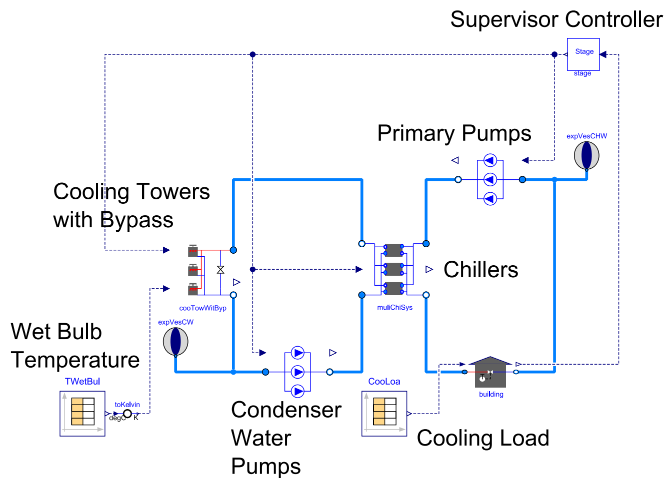

Figure 5 Diagram of the top-level Modelica model for the studied chiller plant

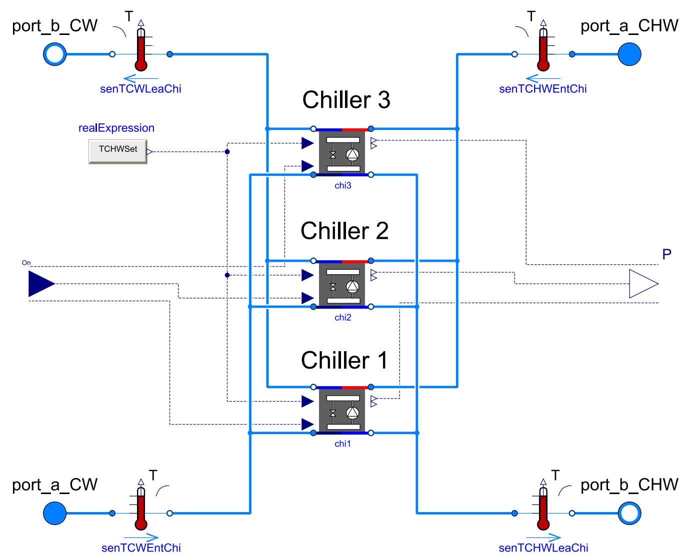

Figure 6 Diagram of the subsystem model for the Chillers

Figure 6 shows the subsystem model for *Chillers*. The three chillers are connected in parallel and each chiller can be started independently. The inputs for this subsystem include the control signal (ON/OFF) for each chiller, the chilled water set point and the temperature of the chilled and condenser water entering the chillers. The output is the power of each chiller. A *Chillers.Carnot* model in the *Buildings* library is used to calculate the power of each chiller:

$$P_{ch} = P_{ch,nom} PLR COP_{nom} / (\frac{T_{eva}}{T_{con} - T_{eva}} \varepsilon_{carnot} \varepsilon_{PLR}(PLR)), \tag{24}$$

where $P_{ch,nom}$ is the nominal power of the chiller, PLR is the partial load ratio, COP_{nom} is the chiller's coefficient of performance at the nominal condition, T_{eva} and T_{con} are the temperatures in the evaporator and condenser sides of the chiller, respectively. In this study, T_{eva} and T_{con} were assumed to be equal to $T_{chw,lea}$ and $T_{cw,ent}$, respectively. The ε_{carnot} is the Carnot effectiveness (assumed to be constant) and ε_{PLR} is the chiller's operation effectiveness at partial loads, which is a function of PLR:

$$\varepsilon_{PLR}(PLR) = c_1 + c_2 PLR + c_3 PLR^2 + (1 - c_1 - c_2 - c_3) PLR^3, \tag{25}$$

where c_1, c_2, c_3 are constant coefficients. In order to mimic the internal capacity control of each chiller, a PI controller was used to modulate PLR for each chiller to maintain $T_{chw,lea}$ as 3.89°C.

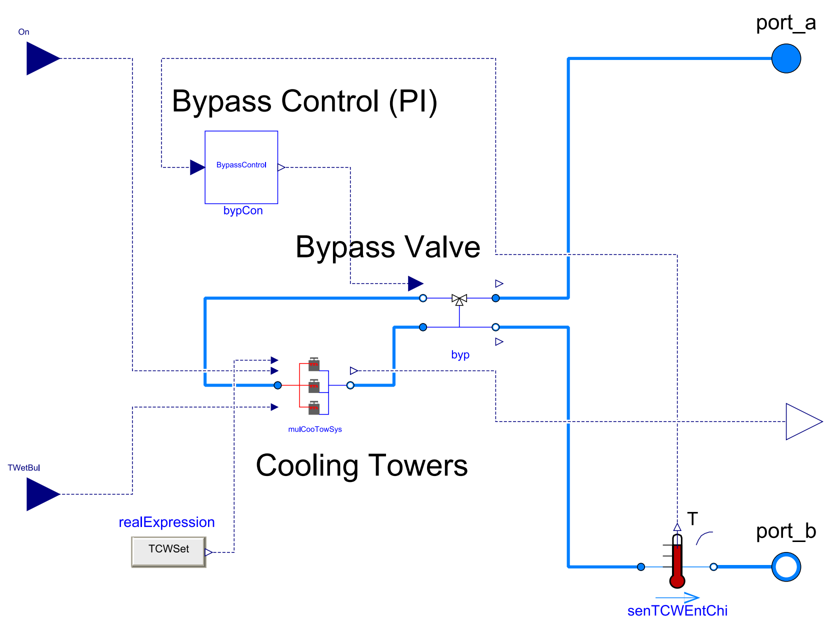

Figure 7 Diagram of the subsystem model for the Cooling Towers with Bypass

Figure 7 shows the diagram of the *Cooling Towers with Bypass* subsystem model. The model inputs include the control signal (ON/OFF) for each cooling tower, the temperature of the condenser water entering the cooling towers, the condenser water set point, and T_{wb}. The outputs are the power of each cooling tower. The bypass valve and the associated control are also included in this model. The cooling tower is modeled with the model *CoolingTowers.YorkCalc* in the *Buildings* library. The model calculates the approach temperature using a purely-empirical YorkCalc correlation [29]. The fan power P_{tw} is computed as

$$P_{tw} = P_{tw,nom} y^3. \tag{26}$$

where y is the fan speed ratio and $P_{tw,nom}$ is the nominal fan power. A PI controller is used to adjust y according to $T_{cw,set}$.

The subsystem model for the *Supervisor Controller* is shown in Figure 8. The core of the *Supervisor Controller* is a state graph model that is in the middle of the model diagram. It consists of state (oval icon) and transition (bar icon) modules. The state modules were used to represent the four states described in Figure 4. The transition module determines when to switch one state to another state. Each transition module has one preceding state and one succeeding state. When the conditions are met, the transition fires.

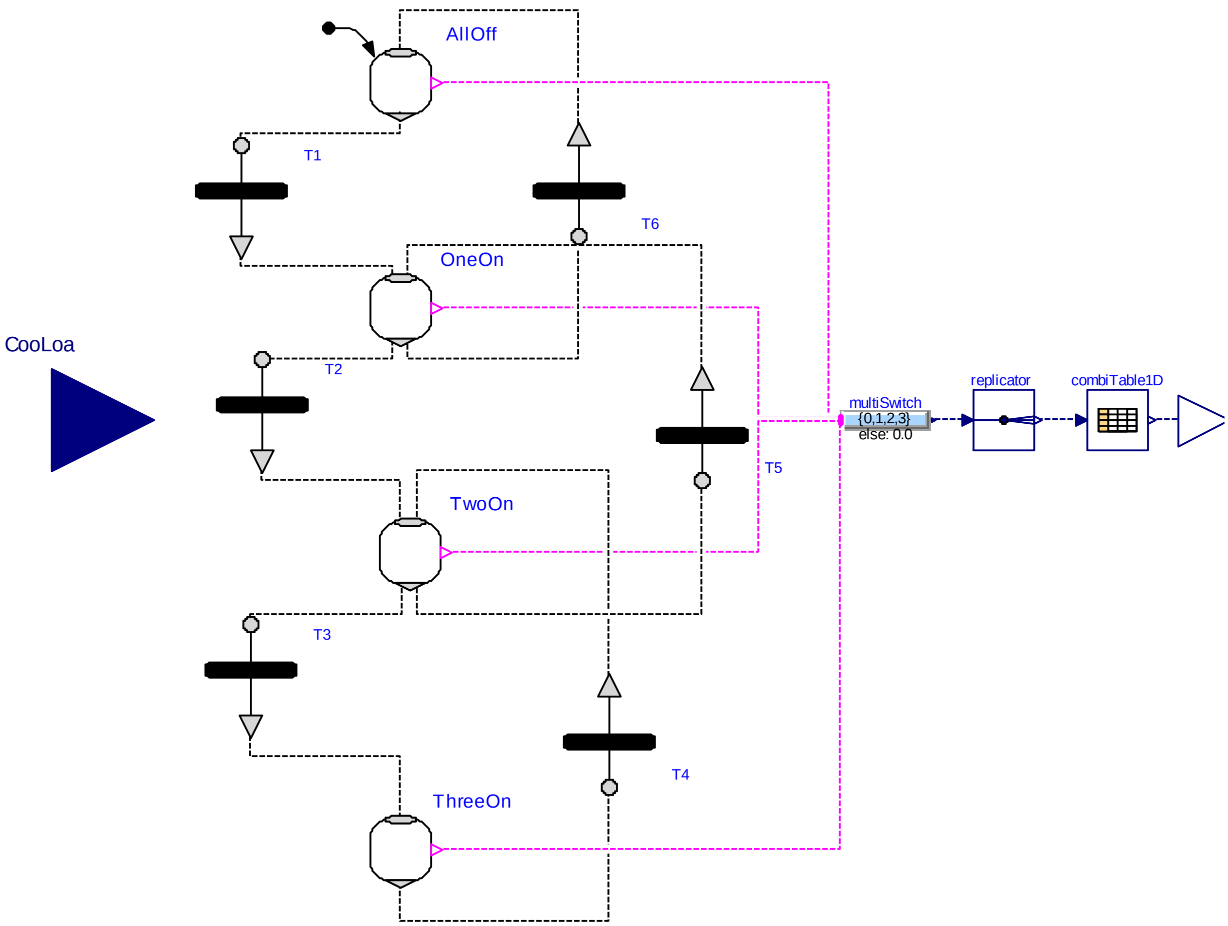

Figure 8 Diagram of the subsystem model for the Supervisor Controller

We calibrated chiller models using one week measured data. In the calibration, we used the temperatures of the condenser and chilled water entering the chillers as input variables. The goal was to minimize the difference between the measured and simulated power of chiller by tuning the coefficients of the chiller performance curve (c_1, c_2, c_3 , c_4 in equation (25)), the nominal condenser water temperature, and the chilled water temperature. Figure 9 shows the calibration result of chiller #1 for one week in 2012. The calibrated model can predict a close result for the temperature of the condenser water leaving the chiller, $T_{cw,lea}$, and the chiller power since the relative errors of most of the predictions are less than 5%.

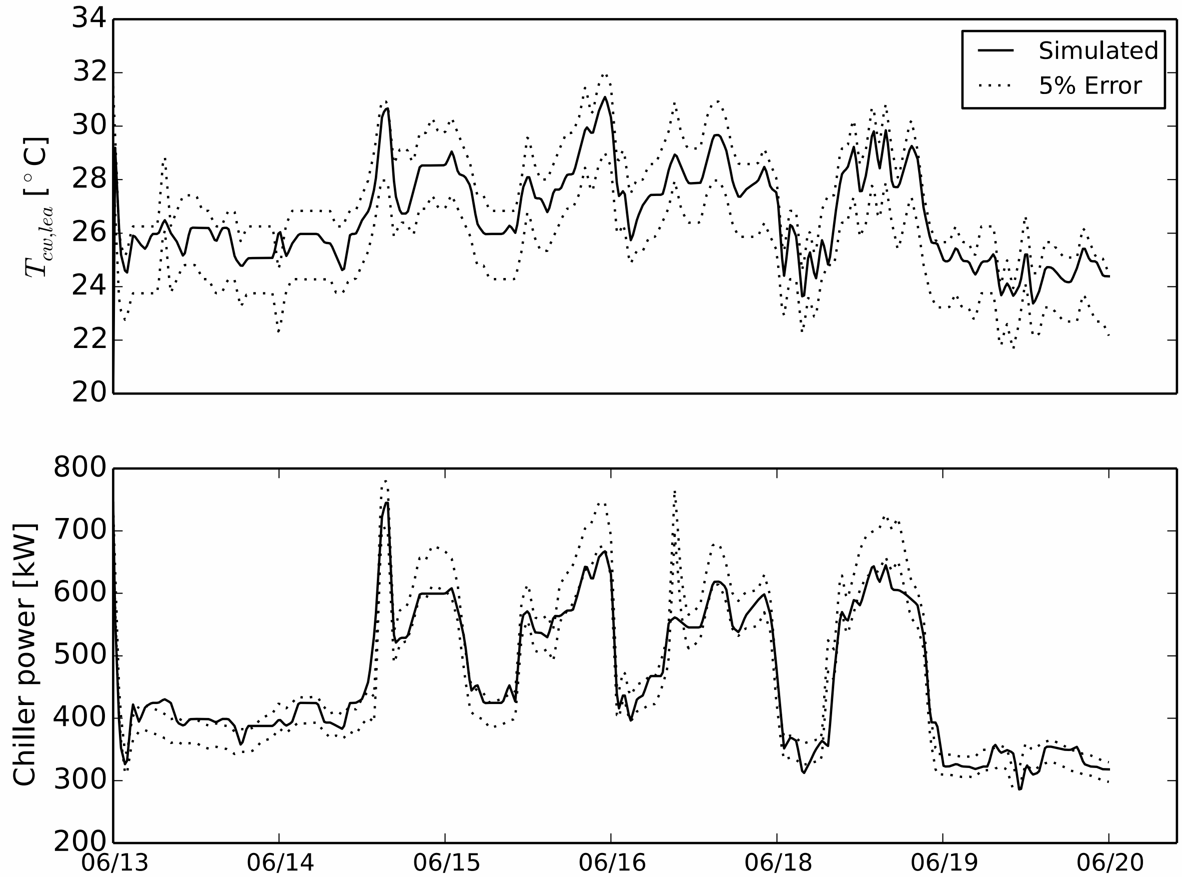

Figure 9 Calibration of the chiller model (chiller #1)

4.3. Optimization Settings

In this study, we used the GenOpt [30] optimization engine and employed the Hooke Jeeves algorithm. Polak [31]). The Hooke Jeeves method was selected because it was very simple to implement, and it did not require information regarding derivatives of the optimization objective functions. Important examples of such implementations include [32],[33], and [34]. The $\{T_1, \ldots, T_n\}$ defined in equation (7) was set to be [15.44, 29.44^{o}C] with an interval of 1^{o}C. We used the historic data for $\dot{Q}$ and T_{wb} as the input variables, which is equivalent to having a perfect prediction model. The perfect prediction model creates an ideal input to avoid uncertainties in optimization inputs while evaluating the optimization method. The optimizations were performed over a period of 1 year. Figure 10 shows the annual hourly $\dot{Q}$ and T_{wb} in the year of 2012. The $\dot{Q}$ was obtained from on-site measurement and T_{wb} was from a nearby weather station [35]. Since both $\dot{Q}$ and T_{wb} were hourly data, they were linearly interpolated during one hour to provide the inputs for the dynamic simulation.

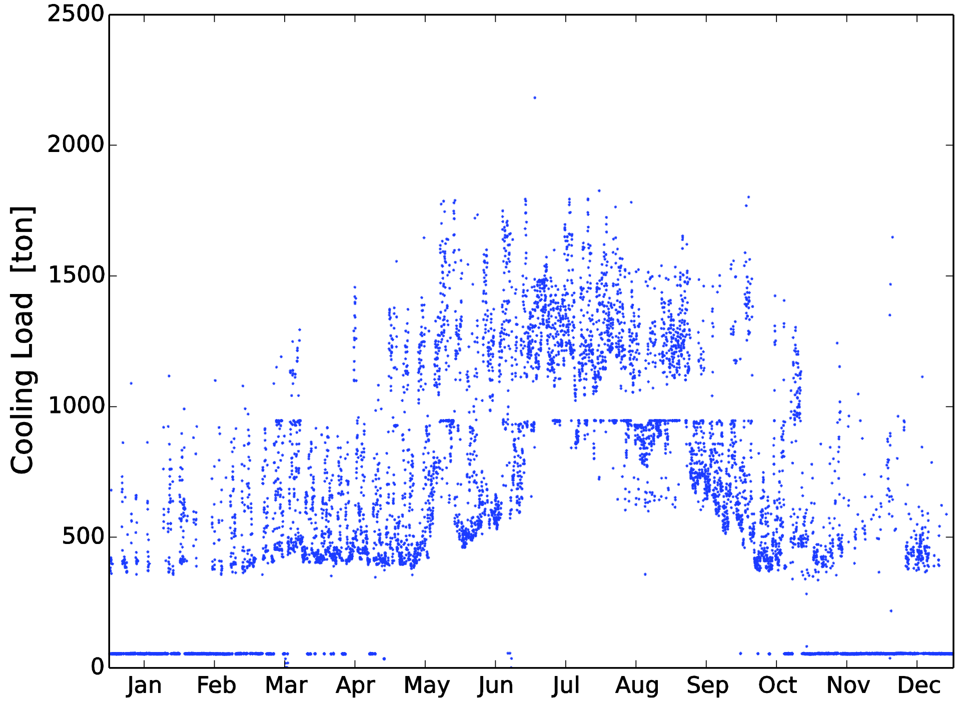

(a)

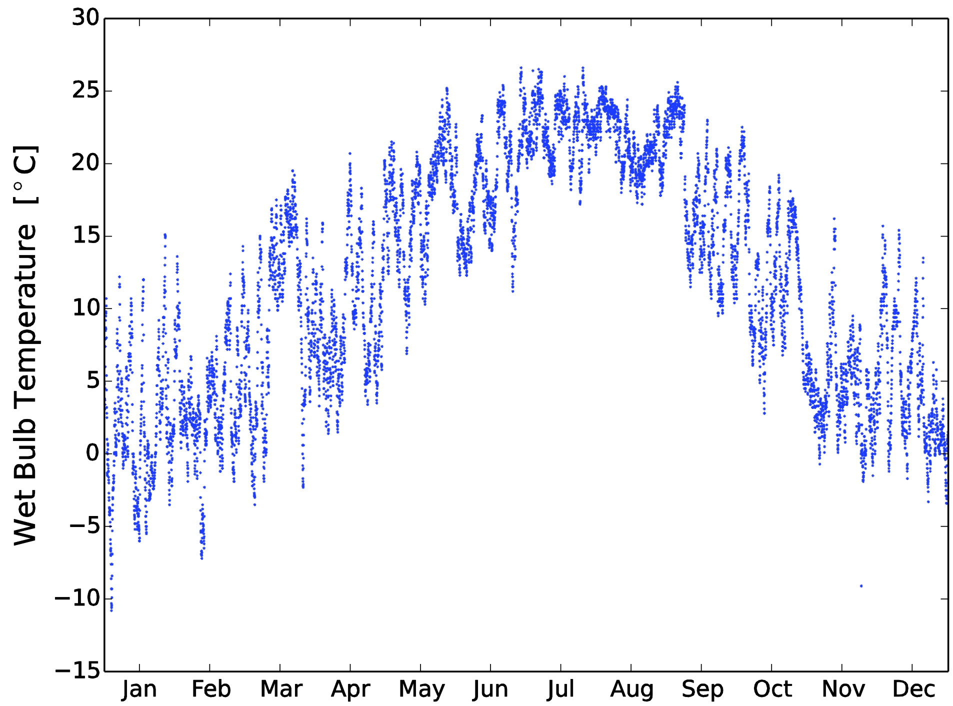

(b)

Figure 10 Input data for the optimziation (a) cooling load (b) wet bulb temperature

To evaluate the impact of the optimization frequency on the energy savings from the condenser water set point optimization, we performed optimizations with three different frequencies: once an hour (*Hourly OPT*), once a day (*Daily OPT*) and once a week (*Weekly OPT*) using historic data as perfect predictions of $\dot{Q}$ and T_{wb}. An exhaustive search method with a frequency as once an hour (*Hourly ES*) was used as the benchmark.

The optimizations were performed using a Dell Precision T7600 Tower Workstation computer with a Four Core XEON processor (E5-2609, 2.4GHz, 10M, 6.4 GT/s). The operation system is Windows 7 Ultimate.

4.4. Evaluation of Starting Point Selection Methods

In this section, we evaluated the performances of four different starting point selection methods. The four methods are: approach temperature, middle point, previous value, and high point. All the four methods are implemented in *Hourly OPT*.

Table 1 shows the accuracy of the optimization with four starting point selection methods compared with the *Hourly ES*. There are 8,760 searches performed for the hourly optimization over a year. None of the starting point selection methods could guarantee the global minimum for all searches. With a better starting point, the search using the approach temperature method could mitigate the local minima problem and had the lowest failure point ratio (the ratio of number of failure searches in finding global optimal to the total number of searches). This means the accuracy of the simple estimation on the approach temperature doesn't significantly impact the searching of the optimal results in this study. The failure ratio of the middle point method and the high point method were about twice of the approach temperature method. The previous value method experienced the highest failure rate, which is more than three times compared to the approach temperature method. This means that the search with the previous value method is more likely trapped by local minima. However, it is surprising that the energy saving penalties for the failures were significantly smaller compared to the searching failure ratios.

Table 1 Comparison of the accuracy using different starting point selection methods

	Approach Temperature	**High Point**	**Previous Value**	**Middle Point**	**Benchmark (Exhaustive Search)**
Number of Failure Searches	315	814	1,080	715	N/A
Failure Search Ratio	3.59%	9.27%	12.30%	8.14%	N/A
Annual Energy Consumption [kWh]	5,028,148	5,030,700	5,030,545	5,028,436	5,027,758
Annual Energy Saving Ratio	9.67%	9.63%	9.63%	9.67%	9.68%

Table 2 compares the computational performances of four methods. Depending on the starting point selection methods, the number of simulations needed by the optimization arranges from 30,989 to 52,285 which is significantly less than 113,658 simulations required by the exhaustive search. In terms of the computing time, the previous value method had the best performance and it reduced the number of simulations by around 72.73% and computing time by about 55.74% compared to the exhaustive search. The approach temperature method had similar performance as the previous value method. The high point method and the middle point method had lower reduction ratios for both the number of simulation (54.00%-57.82%) and computing time (40.40% - 42.25%).

Table 2 Comparison of the computational performance using different starting point selection methods

	Approach Temperature	**High Point**	**Previous Value**	**Middle Point**	**Exhaustive Search**
Number of Simulation	34,585	52,285	30,989	47,941	113,658
Number of Simulation Reduction Ratio	69.57%	54.00%	72.73%	57.82%	N/A
Computing Time [s]	25,045	32,933	24,459	31,914	55,258
Computing Time Reduction Ratio	54.68%	40.40%	55.74%	42.25%	N/A

It is worth mentioning that the average CPU time for each hourly optimization is around 2.86-6.31s, which is significantly less than the optimization period. Thus, we believe that the model and the optimization is fast enough to perform optimization more frequently.

To get more insights on when and why each method failed to find the global minimum, we studied four different scenarios. The first scenario happened when $\dot{Q}$ or T_{wb} was low. In this scenario, the flat range was likely to occur at the high end. As shown in Figure 11 (a), the flat range was between 27.44ºC and 29.44ºC. Since the high point method selected $T_{cw,set,H}$ as 29.44ºC, it was trapped by the local minima within the flat range. Other methods selected a starting point outside the flat range and successfully found the global minimum.

The second scenario occurred when $\dot{Q}$ was extremely low. This could happen in the winter that the chiller was still running to provide cooling for building internal zones, such as computer rooms, even T_{wb} is very low. The flat range extended to a very low temperature (Figure 11(b)) and both the middle point method and high point method failed to find the global minimum.

The third scenario happened when $T_{wb} < T_{wb,nom}$ and $\dot{Q}$ was relatively high. As mentioned earlier, equation (19) may underestimate $T_{cw,low}$. In that case, the approach temperature method will get stuck in the local minima. For instance, in Figure 11 (c), $T_{cw,set,sta}$ given by equation (19) was 24.44ºC, which was still in the flat range of [21.44, 24.44ºC]. Since the initial search step is 2.00ºC, the optimization algorithm found that both $T_{cw,set}$ = 22.44ºC and 26.44ºC cause a higher energy consumption than $T_{cw,set}$ = 24.44ºC, but missed the global minimum at 25.44ºC. In this case, using a smaller initial search step, such as 1.00ºC may avoid the problem. However, this is at the cost of longer searching time.

The fourth scenario appeared when the difference between the optimal $T_{cw,set}$ for the adjacent optimization periods was significant. This made the previous value method fail to reach the global minimum. As shown in Figure 11 (d), the previous value method was stuck at 22.44ºC, which was the optimal $T_{cw,set}$ for the previous optimization period.

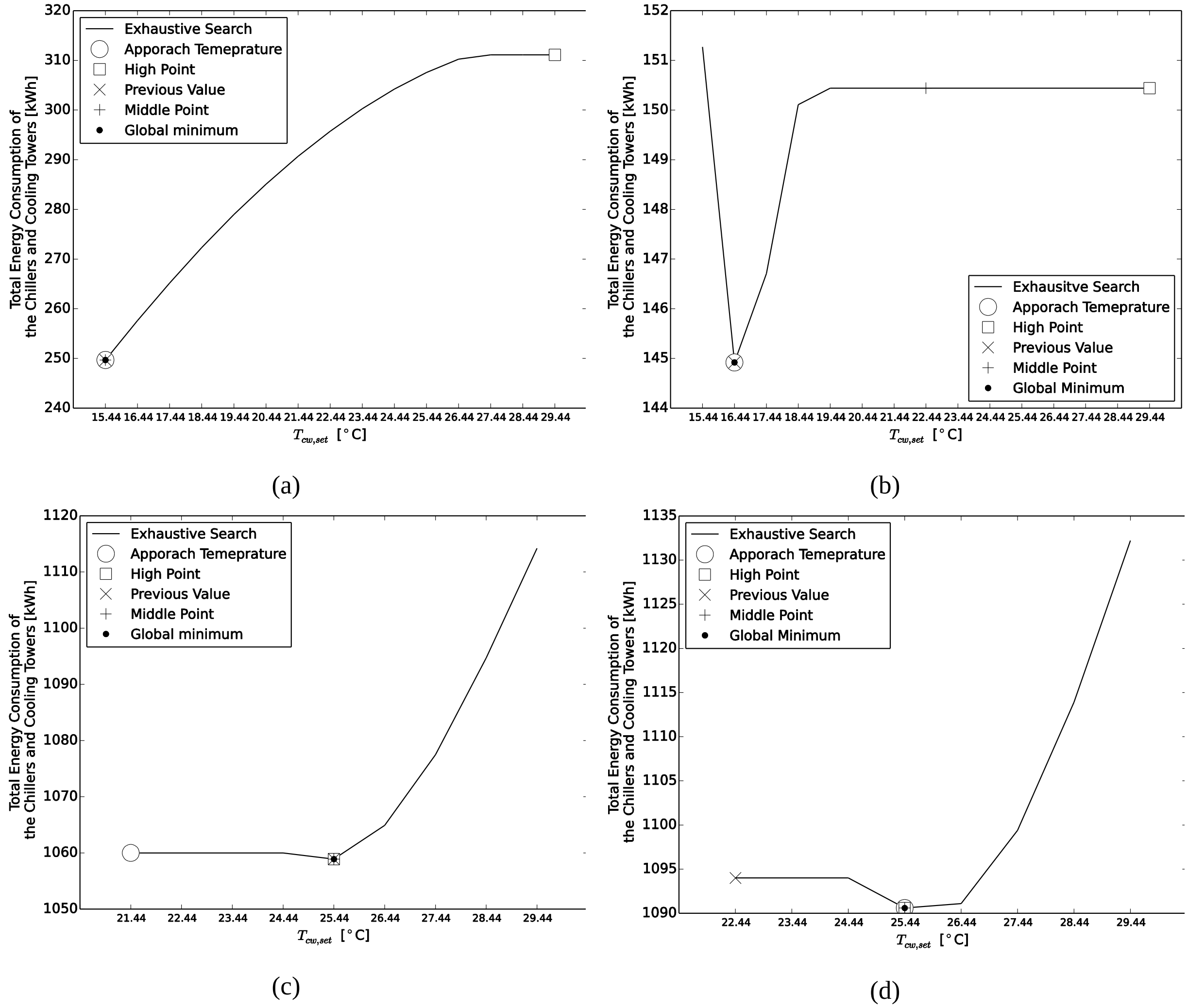

Figure 11 The scenarios when different starting point selection methods failed to find the global minmum

To understand why relatively large searching failure ratios only led to small differences in energy savings, we analyzed the energy saving penalty due to failures in identifying the optimal condenser water set point. Based on Figure 12, for all the methods, more than 90% of the energy saving penalties are less than 5%. As shown in Figure 11, the energy saving penalties can be as low as 0.20%. Thus, although the searching failure ratios of those methods are up to 12.30%, the impact of the searching failures on the total energy savings is not quite significant.

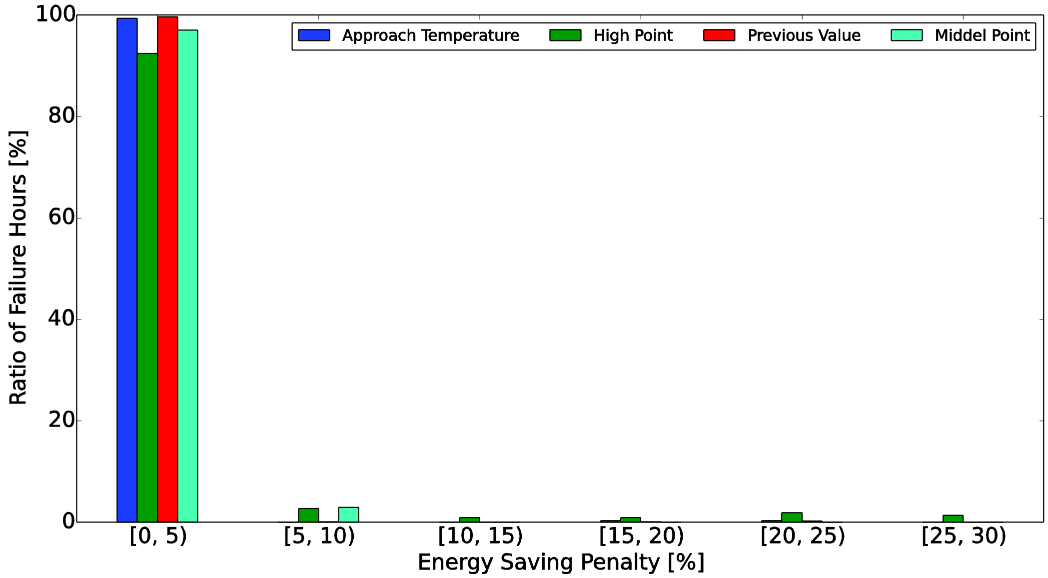

Figure 12 The energy saving penalty due to the failure in predicting the optimal condenser water set point

4.5 Evaluation of the Impact of the Optimization Frequency on the Energy Saving

To model the uncertainties in the load and weather prediction due to long prediction horizons (one day and one week), we used the following equation to generate the synthetic errors:

$$\dot{Q}^* = \dot{Q} + random(-\Delta\dot{Q}\ ,\Delta\dot{Q}), \tag{27}$$

$$T_{wb}{}^* = T_{wb} + random(-\Delta T_{wb}, \Delta T_{wb}) + T_{staerr}, \tag{28}$$

where $\dot{Q}^*$ and $T_{wb}{}^*$ are the predicted cooling load and wet bulb temperature with errors. T_{staerr} is the static error occurs in the wet bulb temperature prediction. For the hourly optimization, we assumed $\Delta\dot{Q} = 0$ W, $\Delta T_{wb} = 0$ K, and $T_{staerr} = 0$ K so that we could use the results of the *Hourly OPT* as the benchmark for comparison. For the daily optimization, $\Delta\dot{Q} = 20\%\dot{Q}_{nom}$, $\Delta T_{wb} = 1$ K, and $T_{staerr} = 1$ K respectively. For the weekly optimization, $\Delta\dot{Q} = 40\%\dot{Q}_{nom}$, $\Delta T_{wb} = 2$ K and $\Delta T_{wb} = 0$ K, and $T_{staerr} = 1$ K. The $random(a, b)$ is a function that returns a random value between the input range [a, b]. A daily optimization and a weekly optimization using the above inputs were named *Daily OPT with Error* and *Weekly OPT with Error*, respectively. The approach temperature starting point selection method was applied in all optimizations.

Table 3 compares the performance of the optimization with different optimization frequencies. The *Hourly OPT* provided almost the same solution as the *Hourly ES* with about half of the computing time. By further reducing the number of optimizations, the *Daily OPT* and the *Weekly OPT* achieved an around 95.00% time and 97.00% reduction in computing time with only 0.07% and 0.09% penalty in predicted energy saving than the *Hourly ES*, respectively. Compared to the *Hourly OPT*, the *Daily Opt* and the *Weekly OPT* were about 10 times and 15 times faster and provides energy savings of only 0.07% less. The reason why the *Daily Opt* and the *Weekly OPT* did not achieve 24 times and 168 times faster than the *Hourly OPT* is because the daily and weekly simulation cost more time to solve than the hourly simulation. Even with uncertainties in the $\dot{Q}$ and T_{wb} prediction, the *Daily OPT with Error* and the *Weekly OPT with Error* got a similar energy savings compared to the *Daily OPT* and the *Weekly OPT.*

Table 3 Perforamnces of different optimization frequencies

	Hourly OPT	**Daily OPT**	**Daily OPT with Error**	**Weekly OPT**	**Weekly OPT with Error**
Annual Energy Consumption [kWh]	5,028,148	5,031,571	5,031,752	5,032,502	5,032,199
Energy Saving Ratio	9.67%	9.60%	9.60%	9.58%	9.59%
Computing Time [s]	25,045	2,536	2,796	1,658	1,912
Computing Time Reduction Ratio	54.68%	95.41%	94.94%	97.00%	96.54%

To understand why the impact of the optimization frequency on the energy savings is not significant, we investigated the profiles of the inputs for the condenser water set point optimization. Figure 13 shows the distribution of the daily and weekly standard deviations in the wet bulb temperature in Washington D.C. in 2012. The standard deviations in the wet bulb temperature of all the days and the weeks are less than 6.00^{o}C. This means the weather of the studied period (year of 2012) in Washington D.C. is relatively temperate with a small variation in the wet bulb temperature. We then looked at the cooling load distribution, since there are different cooling load profiles for different seasons in the cooling period, we selected two typical days with different cooling load profiles: one day is from the mild season (April 20th, Friday) and the other day is from the hot season (July 20th, Friday). Both the mild day and the hot day have the daily standard deviation in the wet bulb temperature less than 6.00^{o}C.

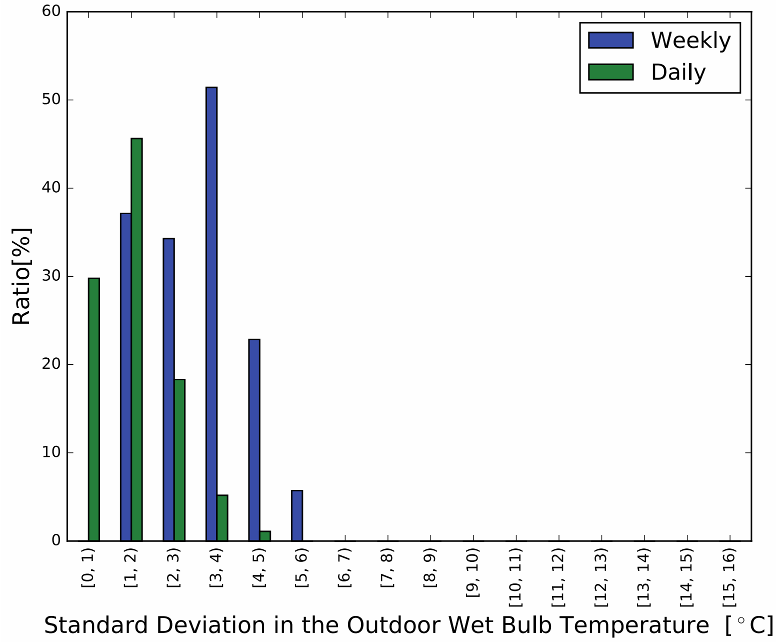

Figure 13 The distribution of the standard deviations for the wet bulb temperature of Washington D.C. in 2012

For the mild day, the cooling load changed from around 400 ton to 900 ton and the wet bulb temperate was from 11.00ºC to 16.00ºC (Figure 14). The *Hourly OPT* predicted the same results as the *Hourly ES* and a 2,648 kWh (16.14%) energy saving was achieved. The *Daily OPT* produced a slightly different result with energy savings of 16.13%. The $T_{cw,set}$ was constant as 15.44ºC from 0:00 to 13:00 because of the low wet bulb temperate. The $T_{cw,set}$ began to increase at 14:00 after T_{wb} passed 15.00ºC. At around 17:00, $T_{cw,set}$ suddenly raised to 20.44ºC. The reason for the quick increase is that at 17:00, the cooling load decreased from 900 ton to 731 ton and the number of operating chillers reduced from 2 to 1. As a result, the cooling load was met by the remained operating chillers. With the increased cooling load, it took more effort for the dedicated cooling tower to cool the condenser water to the given $T_{cw,set}$, which makes the optimal $T_{cw,set}$ increase. After 17:00, $T_{cw,set}$ began to decrease to reflect the reduced cooling load. It returned to 15.44ºC at 19:00 and remained unchanged for the rest time. The *Daily OPT* predicted $T_{cw,set}$ as 15.44ºC and there are only four hours when the $T_{cw,set}$ by the *Daily OPT* and the *Hourly OPT* was different.

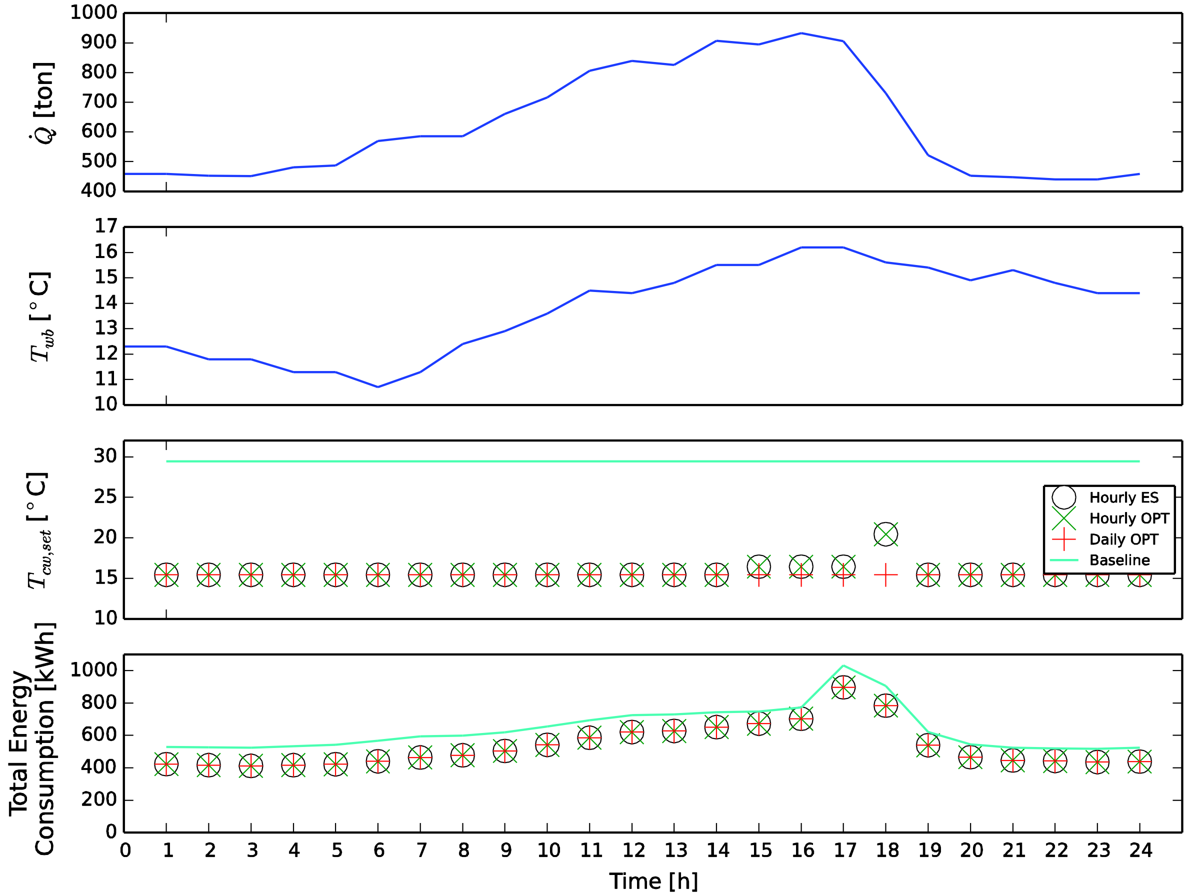

Figure 14 The simulation results for April 20, 2012

As shown in Figure 15, the cooling load and the wet bulb temperate in the hot day were higher than those for the mild day in Figure 14. Again, the *Hour OPT* predicted the same results as the *Hourly ES*. Basically, the trajectory of $T_{cw,set}$ in the *Hourly ES* followed the change of T_{wb} during that day. The *Daily OPT* predicted $T_{cw,set}$ as 21.44ºC. The energy savings from the *Hour OPT* were 682.4 kWh (2.31%) and that for the *Daily OPT* were 681.9 kWh (2.30%). Although there are only three hours when the $T_{cw,set}$ by the *Daily OPT* and the *Hourly OPT* are the same, the differences between the prediction by the *Daily OPT* and the *Hourly OPT* are not larger than 2.00ºC.

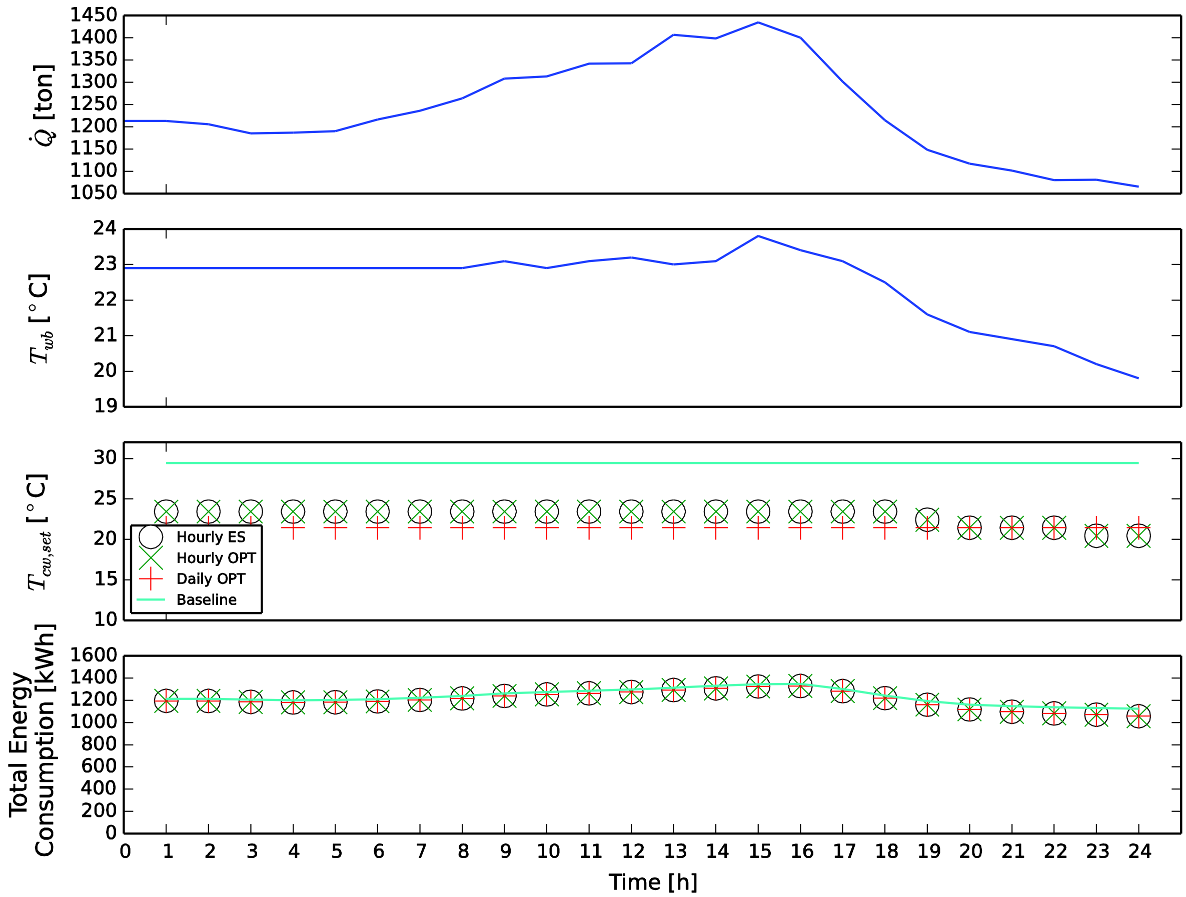

Figure 15 The simulation results for July 20, 2012

Based on the above analysis, we can see that despite of different cooling load profiles, the lower daily deviation in the wet bulb temperature makes the difference between the predictions by the *Daily OPT* and the *Hour OPT* not obvious.

Similarly, the wet bulb temperature does not change significantly over a week so that the *Weekly OPT* could achieve similar performance to the *Daily OPT*. The standard deviations for the weeks, to which April 20 and July 20 belong, are 3.36ºC and 1.81ºC, respectively. As a result, the predictions by the *Weekly OPT* for the two weeks are 15.44ºC and 24.44 ºC, which are both close to the results by the *Daily OPT* for April 20 and July 20, respectively.

5. Conclusion

In this paper, we proposed an operational support system to improve the operational efficiency of condenser water loops in legacy chiller plants. We evaluated how different starting point selection methods and the optimization frequency affect the condenser water set point optimization results via a case study. Based on the results of the case study, the following conclusions can be drawn:

1) The proposed system can achieve significant energy savings for the studied chiller plant. The annual energy saving ratio is up to around 9.67%. It should be noted that the energy savings is reached without adding new equipment or requiring significant efforts for implementation.

2) Optimization starting point selection does not significantly impact energy savings from the condenser water set point optimization for the studied chiller plant significantly, although it does impact the computing time and the failure rate on finding the global optimum. The previous value method can achieve the fastest search but it also obtains the largest failure number. The approach temperature method is promising since it has a failure rate 2-3 times lower than other methods. The computing time of the approach temperature method is almost the same as the previous value method.

3) The optimization frequency doesn't significantly affect the energy savings from the condenser water set point optimization for the studied chiller plant. This is because the daily and weekly variation in the wet bulb temperature is not very large for the site in the studied year, which leads to small differences between the predictions of the optimal condenser water set point with different optimization frequencies.

In this paper, we demonstrated the performance of the operational support system via a single chiller plant with one type of climate condition. It will be interesting to perform more simulations to access the energy saving potential of this approach for different plant configurations, cooling loads, and climates in the future work. As a pilot study, we manually developed the dedicated model for the studied plant and calibrated the models according to the measured data. To enable the large scale application, it is worth investigating how to automatize the procedure for creating and calibrating the chiller plant models so that the efforts for implementation can be minimized.

Acknowledgement

This research was supported by the U.S. Department of Defense under the ESTCP program. The authors thank Marco Bonvini, Michael Wetter, Mary Ann Piette, Jessica Granderson, Oren Schetrit, Rong Lily Hu and Guanjing Lin for the support provided through the research.

This research also emerged from the Annex 60 project, an international project conducted under the umbrella of the International Energy Agency (IEA) within the Energy in Buildings and Communities (EBC) Programme. Annex 60 will develop and demonstrate new-generation computational tools for building and community energy systems based on Modelica, Functional Mockup Interface and BIM standards.

Reference

[1] Westphalen D, Koszalinski S. Energy Consumption Characteristics of Commercial Building HVAC Systems Volume I : Chillers, Refrigerant Compressors,and Heating Systems. Arthur D. Little, Inc.; 2001.
[2] ASHRAE. ASHRAE Handbook HVAC Application. Atlanta: ASHRAE, Inc.; 2011.
[3] Braun JE, Klein SA, Mitchell JW, Beckham WA. Application of optimal control to chilled water systems without storage. ASHRAE Trans 1989;95(1):663-75.
[4] Hydeman M, Zhuo G. Optimizing Chilled Water Plant Control. ASHRAE J 2007;54(3):56-74.
[5] Sun J, Reddy A. Optimal Control of Building HVAC&R Systems using Complete Simulation-based Sequential Quadratic Programming (CSB-SQP). Build Environ 2005;40(5):657-69.
[6] Yu FW, Chan KT. Optimization of Water-cooled Chiller System with Load-based Speed Control. Appl Energ 2008;85(2008):931-50.
[7] Zhang Z, Li H, Turner WD, Deng S. Optimization of the Cooling Tower Condenser Water Leaving Temperature using a Component-based Model. ASHRAE Trans 2011;117(1):934-44.
[8] Malara ACL, Huang S, Zuo W, Sohn MD, Celik N. Optimal Control of Chiller Plants using Bayesian Network. In: Proceedings of The 14th International Conference of the IBPSA Hyderabad, 2015. p. 449-55.
[9] Lu L, Cai W, Soh YC, Xie L, Li S. HVAC System Optimization - Condenser Water Loop. Energ Convers Manage 2004;45(4):613-30.
[10] Ma Z, Wang S, Xu X, Xia F. A Supervisory Control Strategy for Building Cooling Water Systems for Practical and Real Time Applications. Energ Convers Manage 2008;49(8):2324-36.
[11] Lee KP, Cheng TA. A Simulation–optimization Approach for Energy Efficiency of Chilled Water System. Energ Buildings 2012;54(2012):290-6.
[12] Huang S, Zuo W. Optimization of the Water-cooled Chiller Plant System Operation. In: Proceedings of ASHRAE/IBPSA-USA Building Simulation Conference, Atlanta, GA, U.S.A., 2014. p. 300-7.
[13] Ma Y, Borrelli F, Hencey B, Coffey B, Bengea S, Haves P. Model Predictive Control for the Operation of Building Cooling Systems. IEEE Trans Control Syst Technol 2010;20(3):796 - 803.
[14] Lazos D, Sproul A, Ka M. Development of Hybrid Numerical and Statistical Short Term Horizon Weather Prediction Models for Building Energy Management Optimisation. Build Environ;90(2015):82-95.

[15] Huang S, Zuo W, Sohn MD. A Bayesian Network Model for Predicting the Cooling Load of Educational Facilities. In: Proceedings of ASHRAE and IBPSA-USA SimBuild 2016 Building Performance Modeling Conference, Salt Lake City, UT, 2016.
[16] Hassin R, Henig M. Dichotomous Search for Random Objects on an Interval. Math Oper Res 1984;9(2):301-8.
[17] Eiselt HA, Sandblom. Linear Programming and its Applications. 2007 ed. Berlin: Springer-Verlag Berlin Heidelberg; 2007.
[18] Fernandes FP, Costa MFP, Fernandes EMGP, Rocha AMAC. Multistart Hooke and Jeeves Filter Method for Mixed Variable Optimization. In: Proceedings of the 11th international conference of numerical analysis and applied mathematics Rhodes, Greece, 2013. p. 614-7.
[19] Gyorgy A. Efficient Multi-start Strategies for Local Search Algorithms. J Artif Intell Res 2011;41(2011):407-44.
[20] Kelman A, Ma Y, Borrelli F. Analysis of Local Optima in Predictive Control for Energy Efficient Buildings. J Build Perform Simu 2012;6(3):236–55.
[21] Sutherland JW. Analysis of Mechanical Draught Counterflow Air/Water Cooling Towers. J Heat Transfer 1983;105(3):576-83.
[22] Braun JE, Klein SA, Mitchell JW. Effectiveness Models for Cooling Towers and Cooling Coils. ASHRAE Trans 1989;95(2):164-74.
[23] Schwedler M. Effect of Heat Rejection Load and Wet Bulb on Cooling Tower Performance. ASHRAE J 2014;56(1):16-22.
[24] Wetter M, Zuo W, Nouidui T, Pang X. Modelica Buildings library. J Build Perform Simu 2014;7(4):253-70.
[25] Nouidui TS, Phalak K, Zuo W, Wetter M. Validation of the Window Model of the Modelica Buildings Library. In: Proceedings of the 9th International Modelica Conference, Munich, Germany, 2012. p. 727-36.
[26] Zuo W, Wetter M, Li D, Jin M, Tian W, Chen Q. Coupled Simulation of Indoor Enviroment, HVAC and Control System by using Fast Fluid Dynamics and the Modelica Buildings Library. In: Proceedings of ASHRAE/IBPSA-USA Building Simulation Conference, Atlanta, GA, U.S.A., 2014. p. 56-63.
[27] Otter M, Årzén K-E, Dressler I. StateGraph - a Modelica Library for Hierarchical State Machines. In: Proceedings of the 4th International Modelica Conference, Hamburg, Germany, 2005. p. 569-78.
[28] Dassault Systems. Dymola. <http://www.3ds.com/products-services/catia/capabilities/modelica-systems-simulation-info/dymola> (accessed
[29] Input Output Reference: the Encyclopedic Reference to EnergyPlus Input and Output. <http://apps1.eere.energy.gov/buildings/energyplus/pdfs/inputoutputreference.pdf> (accessed May 14. 2015).
[30] Wetter M. GenOpt - a Generic Optimization Program. In: Proceedings of the 7th IBPSA Conference, Rio de Janeiro, Brazil, 2001. p. 601-8.
[31] Polak E. Optimization. Algorithms and consistent approximations. Appl Math Sci 1997;124(
[32] Wetter M, Polak E. Building design optimization using a convergent pattern search algorithm with adaptive precision simulations. Energ Buildings 2005;37(6):603-12.
[33] Coffey B. Approximating model predictive control with existing building simulation tools and offline optimization. J Build Perform Simu 2013;6(3):220-35.
[34] Bagirov AM, Barton AF, Mala-Jetmarova H, Nuaimat AA, Ahmed ST, Sultanova N, et al. An algorithm for minimization of pumping costs in water distribution systems using a novel approach to pump scheduling. Mathematical and Computer Modelling 2013;67(3-4):873-86.
[35] National Climatic Data Center. Quality Controlled Local Climatological Data. <http://www.ncdc.noaa.gov/data-access/land-based-station-data/land-based-datasets/quality-controlled-local-climatological-data-qclcd> (accessed May 14. 2015).